

Online Supplement

Candidate Genes and Mechanisms for 2-Methoxyestradiol-Mediated Vasoprotection

Federica Barchiesi^{*}, Eliana Lucchinetti[†], Michael Zaugg[†], Omolara O Ogunshola^{φ¶},
Matthew Wright[‡], Markus Meyer[‡], Marinella Rosselli^{*}, Sara Schaufelberger^{*}, Delbert G
Gillespie[§], Edwin K Jackson^{§#}, Raghendra K Dubey^{§*¶#}

^{*}Department of Obstetrics and Gynecology, Clinic for Reproductive Endocrinology, University Hospital Zurich; ^φ Institute of Veterinary Physiology, Vetsuisse faculty, Zurich, Switzerland and [¶]Zurich Center for Integrative Human Physiology (ZIHP), University of Zurich, Zurich, Switzerland; [‡]Metabolic and Vascular Disease, Bld 70/411, F Hoffmann La Roche, Basel, Switzerland; [§]Center for Clinical Pharmacology, Departments of Medicine and of [#] Pharmacology and Chemical Biology, University of Pittsburgh School of Medicine, USA; [†]Department of Anesthesiology & Pain Medicine, University of Alberta and Cardiovascular Research Centre, University of Alberta, Edmonton (Canada)

Running Title: SMC Genes Regulated by 2-methoxyestradiol

Corresponding Author Address:

Dr. Raghendra K. Dubey
Department of Obstetrics and Gynecology
Clinic for Reproductive Endocrinology (NORD-1, D217)
University Hospital Zurich
Zurich, 8091-CH
Switzerland
Tel: 41-1-255-8608
Fax: 41-1-255-4439
E-mail: Raghendra.dubey@usz.ch

Supplementary Materials and Methods

Cell Culture. Human (female) aortic smooth muscle cells (HASMCs; 6th to 8th passage; Cascade Biologics Inc) were cultured under standard tissue culture conditions (37°C, 5% CO₂) in M231 culture medium containing smooth muscle cell growth supplement (Cascade Biology Inc, Switzerland).

Microarray Experiments and Analysis. HASMCs grown to subconfluence were treated with either vehicle or 3 μ M 2-ME in the presence of 5% fetal calf serum for 4 hrs (acute phase response/early gene induction) and for 30 hrs (late phase). Following treatment with 2-ME for the prescribed times the cells were washed with PBS and processed for total RNA isolation.

RNA Isolation, cDNA Synthesis, and Microarray Hybridization. Total RNA was extracted from vehicle-treated and 2-ME-treated samples using RNeasy Mini kit (Qiagen) according to manufacturer's instruction. The quality of the isolated RNA was determined with a NanoDrop ND 1000 (NanoDrop Technologies, Delaware, USA) and a Bioanalyzer 2100 (Agilent, Waldbronn, Germany). Only the samples with a 260 nm/280 nm ratio between 1.8–2.1 and a 28S/18S ratio within 1.5–2.0 were further processed. Total RNA samples (2 μ g) were reverse-transcribed into double-stranded cDNA, which was subsequently in vitro transcribed in presence of biotin-labeled nucleotides using a IVT Labeling Kit (Affymetrix Inc., Santa Clara, CA). The labeled cRNA was purified and quantified using BioRobot Gene Exp - cRNA Target Prep (Qiagen AG, Switzerland).¹ Biotin-labeled cRNA samples (15 μ g) were fragmented to 35–200 bp at 94°C in fragmentation buffer (Affymetrix Inc.) and were mixed in 300 μ l of hybridization buffer containing a hybridization control cRNA and control Oligo B2 control (Affymetrix), 0.1 mg/ml herring sperm DNA and 0.5 mg/ml acetylated bovine serum albumin in 2-(4-morpholino)-ethane sulfonic acid (MES) buffer, pH 6.7, before hybridization to GeneChip® Human Genome U_133 Plus 2.0 arrays for 16 h at 45°C. Arrays were then washed using an Affymetrix Fluidics Station 450 EukGE-WS2v5_450 protocol. An Affymetrix GeneChip Scanner 3000 (Affymetrix Inc.) was used to measure the fluorescent intensity emitted by the labelled target.

Microarray Analysis. Normalization and computation of expression values was performed using the Robust Multichip Average algorithm¹. The expression data were analyzed both at the single gene level and at the pathway level as previously described². In a first step, the statistically most relevant differentially regulated transcripts are identified using Significance Analysis of Microarrays³, a method that provides a ranking of the transcripts found to be differentially regulated between any two given protocols. Statistical significance is measured by the q-value, which is the lowest false discovery rate (= percent of genes that are expected to be identified by chance) at which a gene is described as significantly regulated. In a second step, the association between 2-ME treatment and functionally-related group of genes and pathways was studied using Gene Set Enrichment Analysis⁴. Gene Set Enrichment Analysis (GSEA) is a computational method that determines whether an a priori defined set of genes shows statistically significant, concordant differences between two biological states (“phenotypes”). Results are ranked by their normalized enrichment score (NES); a p-value, and the false discovery rate (q-value). Pathway information and references are available at The Molecular Signatures Database

(<http://www.broad.mit.edu/gsea/msigdb>), which is a searchable online collection of gene sets used with GSEA. Several pathways related to atherosclerosis and/or ischemic heart disease were manually created⁵⁻⁷.

Cloning and Protein Expression of Ligand Binding Domains of PPARs. Bacterial and mammalian expression vectors were constructed to produce glutathione-s-transferase (GST) and Gal4 DNA binding domain proteins fused to the ligand binding domains (LBD) of human PPAR δ (aa 139 to 442), mouse PPAR γ (aa 174 to 476) and human PPAR α (aa 167 to 469). Induction, expression, and purification of GST-LBD fusion proteins were performed in *E. coli* strain BL21(pLysS) by standard methods.⁸

PPAR Binding Assay. As described before⁸, scintillation proximity assays were used to determine if 2ME could bind PPARs and displace a high affinity radioligand.

PPAR δ receptor binding was assayed in HNM10 (50mM Hepes, pH 7.4, 10 mM NaCl, 5mM MgCl₂, 0.15 mg/ml fatty acid-free BSA and 15 mM DTT). For each 96 well reaction a 500 ng equivalent of GST-PPAR δ -LBD fusion protein and radioligand, e.g. 20000 dpm {2-methyl-4-[4-methyl-2-(4-trifluoromethyl-phenyl)-thiazol-5-yl-ditritiomethylsulfonyl]-phenoxy}-acetic acid, was bound to 10 μ g SPA beads (Pharmacia Amersham) in a final volume of 50 μ l by shaking. The resulting slurry was incubated for 1h at RT and centrifuged for 2 min at 1300g. The supernatant containing unbound protein was removed and the semidry pellet containing the receptor-coated beads was resuspended in 50 μ l of HNM. Radioligand was added and the reaction incubated at RT for 1h and scintillation proximity counting performed in the presence of test compounds was determined. All binding assays were performed in 96 well plates and the amount of bound ligand was measured on a Packard TopCount using OptiPlates (Packard). Dose response curves were done in triplicates within a range of concentration from 10⁻¹⁰ M to 10⁻⁴ M. IC₅₀ values were calculated using the XLfit program (ID Business Solutions Ltd. UK).

PPAR α receptor binding was assayed in TKE50 (50mM Tris-HCl, pH 8, 50 mM KCl, 2mM EDTA, 0.1 mg/ml fatty acid-free BSA and 10 mM DTT). For each 96 well reaction an 140 ng equivalent of GST-PPAR α -LBD fusion protein was bound to 10 μ g SPA beads (PharmaciaAmersham) in a final volume of 50 μ l by shaking. The resulting slurry was incubated for 1h at RT and centrifuged for 2 min at 1300g. The supernatant containing unbound protein was removed and the semidry pellet containing the receptor-coated beads was resolved in 50 μ l of TKE. For radioligand binding e.g. 10000 dpm of 2(S)-(2-benzoyl-phenylamino)-3-{4-[1,1-ditritio-2-(5-methyl-2-phenyl-oxazol-4-yl)-ethoxy]-phenyl} propionic acid or 2,3-ditritio-2(S)-methoxy-3-{4-[2-(5-methyl-2-phenyl-oxazol-4-yl)-ethoxy]-benzo[b]thiophen-7-yl}-propionic acid in 50 μ l were added, in presence or absence of test compounds and the reaction incubated at RT for 1h and scintillation proximity counting performed. All binding assays were performed in 96 well plates and the amount of bound ligand measured on a Packard TopCount using OptiPlates (Packard). Nonspecific binding was determined in the presence of 10⁻⁴ M unlabelled compound. Dose response curves were done in triplicates within a range of concentration from 10⁻¹⁰ M to 10⁻⁴ M. IC₅₀ values were calculated using the XLfit program (ID Business Solutions Ltd. UK).

PPAR γ receptor binding was assayed in TKE50 (50mM Tris-HCl, pH 8, 50 mM KCl, 2mM EDTA, 0.1 mg/ml fatty acid-free BSA and 10 mM DTT). For each 96 well reaction an 140 ng equivalent of GST-PPAR γ -LBD fusion protein was bound to 10 μ g SPA beads (PharmaciaAmersham) in a final volume of 50 μ l by shaking. The resulting slurry was incubated for 1h at RT and centrifuged for 2 min at 1300g. The supernatant containing unbound protein was removed and the semidry pellet containing the receptor-coated beads was resolved in 50 μ l of TKE. For radioligand binding e.g. 10000 dpm 2(S)-(2-benzoyl-phenylamino)-3-{4-[1,1-ditritio-2-(5-methyl-2-phenyl-oxazol-4-yl)-ethoxy]-phenyl}-propionic acid in 50 μ l were added, the reaction incubated at RT for 1h and scintillation proximity counting performed. All binding assays were performed in 96 well plates and the amount of bound ligand measured on a Packard TopCount using OptiPlates (Packard). Nonspecific binding was determined in the presence of 10^{-4} M unlabelled compound. Dose response curves were done in triplicates within a range of concentration from 10^{-10} M to 10^{-4} M. IC₅₀ values were calculated using the XLfit program (ID Business Solutions Ltd. UK).

PPAR Luciferase Reporter Assay. Baby hamster kidney cells (BHK21 ATCC CCL10) were grown in DMEM medium containing 10% FBS at 37 °C in a 95% O₂:5% CO₂ atmosphere. Cells were seeded in 6 well plates at a density of 10⁵ Cells/well and then batch-transfected with either the pFA-PPAR δ -LBD, pFA-PPAR γ -LBD or pFA-PPAR α -LBD expression plasmids plus a reporter plasmid (pFR-luc luciferase reporter plasmid; Stratagene). Transfection was accomplished with the Fugene 6 reagent (Roche Molecular Biochemicals) according to the suggested protocol. Six hours following transfection, the cells were harvested by trypsinization and seeded in 96 well plates at a density of 10⁴ cells/well. After 24 hours to allow attachment of cells, the medium was removed and replaced with 100 μ l of phenol red-free medium containing the test substances or control ligands (final DMSO concentration: 0.1%). Following incubation of the cells for 24 hours with substances, 50 μ l of the supernatant was discarded and then 50 μ l of Luciferase Constant-Light Reagent (Roche Molecular Biochemicals) to lyse the cells and initiate the luciferase reaction was added. Luminescence for luciferase was measured in a Packard TopCount. Transcriptional activation in the presence of a test substance was expressed as fold-activation over cells incubated in the absence of the substance. EC₅₀ values were calculated using the XLfit program (ID Business Solutions Ltd. UK).

Hypoxic Experiments and Inhibitor Treatment. For hypoxic experiments HASMCs were exposed to 1% O₂ for 2 hrs in a purpose-built glove-box chamber (In vivo 400, RUSKINN Technologies, Guiseley, UK) maintained at 37°C with 5% CO₂. Normoxic control cultures were maintained at 21% O₂. 2-ME (0.5-1 μ M) was added to the cultures immediately prior to hypoxic exposure.⁹

Western Blot. Cells were lysed in lysis buffer (150 mM NaCl, 50 mM Tris, 1% Triton X-100, 1% NP-40) for 10 min and centrifuged at 16,000 rcf for 10 min (4°C) and the supernatant collected. 50 μ g of protein were loaded on SDS-polyacrylamide gels and transferred to nitrocellulose membranes. Membranes were incubated anti Hif-1 α (NB 100-479, 1:1000, NOVUS, Littleton, USA) and anti β -actin (Sigma, 1:5000). Following washes, membranes were incubated with a secondary HRP-conjugated antibody for 1 h at room temperature. All blots were normalised to β -actin and normoxic controls and at least 3

independent experiments were performed. Results were quantified by densitometry using Image J software (NIH, Bethesda, USA).

Immunocytochemistry: HASMCs were grown on coverslips in 24 well plates then subjected to hypoxia (1% O₂) for 2 hrs. Cultures were fixed with 4% paraformaldehyde in PBS (pH 7.4) for 5 min at room temperature then permeabilized in 0.1% Triton X-100 for 1 min and blocked with 10% normal goat. Cells were then incubated with primary antibodies overnight at 4°C and secondary antibody AlexaFluor 488 (Molecular Probes, Leiden, Netherlands) for 1 h at room temperature. Coverslips were then washed and mounted. Slides were viewed and analysed using an Axiovert inverted fluorescent Microscope (Zeiss, Germany).¹⁰

Cell growth, viability, aneuploidy and Apoptosis studies:

Growth Studies: [³H]Thymidine incorporation (index of DNA synthesis), [³H]proline incorporation (index of collagen synthesis) and cell proliferation were conducted as previously described¹¹. HASMCs were exposed to various treatments for 24 hours (thymidine incorporation studies), 48 hours (proline incorporation studies) or 5 days (cell proliferation studies).

Viability : Trypan blue exclusion assay was employed to assess the effects of 2-ME on SMC viability. Briefly, SMCs grown to sub-confluence in multiwell slides in presence of 5% serum were incubated for 36 hours in presence or absence of 2-ME (0.001 – 10 µmol/L) in DMSO (final DMSO concentration 1µl DMSO/ml medium). Subsequently, the medium was removed and medium together with 0.4% trypan blue at 1:1 ratio added and the cells incubated for 3 min. Subsequently, the total cells and the number of dead cells, identified as cells which take up trypan blue counted microscopically.

As an additional test for the effects of 2-ME on HASMC viability, growing cells were treated with 2-ME for 48 hrs and subsequently the treatment was withdrawn and cells grown for another 48 hrs and cell count performed.

Apoptosis : We have previously shown that 2-ME does not induce apoptosis in HASMCs. To further confirm our findings we conducted additional studies using other markers for apoptosis. In this context we assessed the impact on DNA fragmentation, Caspase 7 fragmentation and apoptotic vesicle formation (using DAPI staining).

DNA-Fragmentation: We investigated a potential apoptotic effect of 2-ME on the long term. Briefly, for DNA fragmentation HASMC grown in serum containing medium were treated with 0.1, 1 and 5 µM 2-ME for 7 days, changing the treatment every 2 days. DNA was isolated and run on a gel and apoptotic DNA fragmentation visualized. Caspase-7 fragmentation: Since caspase-7 is an effector caspase involved in the intrinsic as well in the extrinsic apoptotic pathway. Hence we assessed the effects of 2-ME on its expression and fragmentation. HASMCs were treated with or without 2-ME (1-10 µmol/L) or H₂O₂ (a known inducer of apoptosis; 8mmol/L) for 24 hrs. Subsequently, the cells were washed and lysed and Western blotting conducted to assess caspase-7 fragmentation.

Aneuploidy studies: To assess whether 2-ME induces aneuploidy in HASMCs we conducted flow cytometric analysis following propidium iodide staining to identify 8N cell

population and DAPI staining to identify multinucleated cells microscopically. Because 2-Me has been shown to induce differential effects in various cells, we used Glial cells as a positive control. Briefly, subconfluent HASMCs or Glial cells were treated with 0-10 $\mu\text{mol/L}$ of 2-ME for 48 hrs and subsequently stained with either propidium iodide following trypsinization and fixation and the distribution of 2-N, 4-N or 8-N cell population analyzed by flowcytometry. For microscopic analysis the cells were fixed following the respective treatments and stained with DAPI. The multinucleated cells were identified microscopically.

References:

1. Irizarry RA, Bolstad BM, Collin F, Cope LM, Hobbs B, Speed TP. Summaries of Affymetrix GeneChip probe level data. *Nucleic Acids Res.* 2003;31:e15.doi:10.1093/nar/gng015.
2. Lucchinetti E, Hofer CK, Bestmann L, Hersberger M, Feng J, Zhu M, Furrer L, Schaub MC, Tavakoli R, Genoni M, Zollinger A, Zaugg M. Gene regulatory control of myocardial energy metabolism predicts postoperative cardiac function in patients undergoing off-pump coronary artery bypass graft surgery: Inhalational versus intravenous anesthetics. *Anesthesiology.* 2007;106:444-457.
3. Tusher VG, Tibshirani R, Chu G. Significance analysis of microarrays applied to the ionizing radiation response. *Proc Natl Acad Sci U S A.* 2001;98:5116-5121.
4. Subramanian A, Tamayo P, Mootha VK, Mukherjee S, Ebert BL, Gillette MA, Paulovich A, Pomeroy SL, Golub TR, Lander ES, Mesirov JP. Gene set enrichment analysis: a knowledge-based approach for interpreting genome-wide expression profiles. *Proc Natl Acad Sci U S A.* 2005;102:15545-15550.
5. Satterthwaite G, Francis SE, Suvarna K, Blakemore S, Ward C, Wallace D, Braddock M, Crossman D. Differential gene expression in coronary arteries from patients presenting with ischemic heart disease: further evidence for the inflammatory basis of atherosclerosis. *Am Heart J.* 2005;150:488-499.
6. Archacki SR, Angheloiu G, Tian XL, Tan FL, DiPaola N, Shen GQ, Moravec C, Ellis S, Topol EJ, Wang Q. Identification of new genes differentially expressed in coronary artery disease by expression profiling. *Physiol Genomics.* 2003;15:65-74.
7. Papaspyridonos M, Smith A, Burnand KG, Taylor P, Padayachee S, Suckling KE, James CH, Greaves DR, Patel L. Novel candidate genes in unstable areas of human atherosclerotic plaques. *Arterioscler Thromb Vasc Biol.* 2006;26:1837-1844.
8. Ausubel FM. Current Protocols in Molecular Biology Edited by :Ausubel Brent R, Kingston RE, Moore DD, Seidman JG, Smith JA, Struhl K. 1987, Wiley Press, New York, USA.
9. Schmid-Brunclik N, Burgi-Taboada C, Antoniou X, Gassmann M, Ogunshola OO. Astrocyte responses to injury: VEGF simultaneously modulates cell death and proliferation. *Am J Physiol Regul Integr Comp Physiol.* 2008;295(3):R864-R873.
10. Ahmad Al A, Gassmann M, Ogunshola OO. Maintaining blood-brain barrier integrity: pericytes perform better than astrocytes during prolonged oxygen deprivation. *J Cell Physiol.* 2009;218:612-622.
11. Dubey RK, Gillespie DG, Zacharia LC, Imthurn B, Jackson EK, Keller PJ. Clinically used estrogens differentially inhibit human aortic smooth muscle cell growth and MAP kinase activity. *Arterioscler Thromb Vas Biol.* 2000;20:964-972.

Supplementary Table S1: Genes regulated by short-term (4 hours) 2-ME treatment identified by Significance Analysis of Microarrays.

Probeset	Gene product	FC	q-value (%)	localFDR (%)
225803_at	F-box protein 32	1.53	97.76	100
210890_x_at	killer cell immunoglobulin-like receptor, two domains, long cytoplasmic tail, 1	1.37	97.76	100
207897_at	corticotropin releasing hormone receptor 2	1.35	97.76	100
227893_at	chromosome 9 open reading frame 130	1.30	97.76	100
216262_s_at	TGFB-induced factor 2 (TALE family homeobox)	1.30	97.76	100
234699_at	ribonuclease, RNase A family, 7	1.31	97.76	100
224137_at	calcium channel, voltage-dependent, gamma subunit 7	1.29	97.76	100
1555345_at	solute carrier family 38, member 4	1.30	97.76	100
225345_s_at	F-box protein 32	1.40	97.76	100
220611_at	disabled homolog 1 (Drosophila)	1.38	97.76	100

Probeset represent the probe identifier as defined by Affymetrix, FC=fold change; q-value (%)=lowest false discovery rate at which a gene is described as significantly regulated; localFDR (%)=false discovery rate.

Supplementary Table S2: Top 20 down-regulated genes by prolonged (30 hours) 2-ME treatment identified by Significance Analysis of Microarrays.

Probeset	Gene product	FC	q-value (%)	Local FDR (%)	Further information
219918_s_at	asp (abnormal spindle)-like, microcephaly associated	0.58	0	32.0	It is essential for normal mitotic spindle function in embryonic neuroblasts. However, it is widely expressed in fetal and adult tissues and upregulated in malignant cells.
207828_s_at	centromere protein F, 350/400ka (mitosin)	0.57	0	32.0	Cenp-F is a nuclear matrix component that localizes to kinetochores during mitosis and is then rapidly degraded after mitosis. It is required for kinetochore-microtubule interactions and spindle checkpoint function.
229490_s_at	IQ motif containing GTPase activating protein 3	0.55	0	33.8	IQGAP3 regulates the organization of the cytoskeleton under the regulation of Rac1 and CDC42 (cell division cycle 42).
201292_at & 201291_s_at	topoisomerase (DNA) II alpha 170kDa	0.62	0	33.8	Enzyme that controls and alters the topologic states of DNA during transcription.
209891_at	spindle pole body component 25 homolog (<i>S. cerevisiae</i>)	0.56	0	33.9	Component of the four-protein Ndc80 complex, an essential kinetochore component conserved from yeast to humans, which plays an indispensable role in proper chromosome alignment and segregation during mitosis.
1552619_a_at & 222608_s_at	anillin, actin binding protein (scraps homolog, <i>Drosophila</i>)	0.67	0	34.1	Anillin, one of the first factors recruited to the cleavage site during cytokinesis, interacts with actin, myosin II and septins, and is essential for proper organization of the actomyosin contractile ring.

205046_at	centromere protein E, 312kDa	0.70	0	34.3	Centromere-associated protein E is a kinesin-like motor protein that accumulates in the G2 phase of the cell cycle. It interacts with cenp-f.
228323_at	cancer susceptibility candidate 5	0.63	0	34.5	Kinetochores proteins in <i>C. elegans</i> and yeast have sequence homology to CASC5 and it was shown that CASC5 is localized in kinetochores in a human cancer cell line.
218755_at	kinesin family member 20A	0.67	0	34.5	Kinesin superfamily proteins have been shown to transport organelles, protein complexes and mRNAs to specific destinations along microtubules
209408_at	kinesin family member 2C	0.68	0	34.6	
219306_at	kinesin family member 15	0.63	5.2	34.6	
218009_s_at	protein regulator of cytokinesis 1	0.71	5.2	34.6	This gene encodes a protein that is involved in cytokinesis. The encoded protein is located in the nucleus during interphase, and becomes associated with mitotic spindles in a highly dynamic manner during mitosis, and localizes to the cell mid-body during cytokinesis.
202870_s_at	CDC20 (cell division cycle 20) homolog (<i>S. cerevisiae</i>)	0.71	5.2	34.6	CDC20 appears to act as a regulatory protein interacting with several other proteins at multiple points in the cell cycle.
202705_at	cyclin B2	0.69	5.2	34.6	The B-type cyclins, B1 and B2, associate with p34cdc2 and are essential components of the cell cycle regulatory machinery. B1 and B2 differ in their subcellular localization. Cyclin B1 co-localizes with microtubules, whereas cyclin B2 is primarily associated with the Golgi region.
214710_s_at	cyclin B1	0.73	5.2	34.6	
228273_at	Hypothetical protein FLJ11029	0.70	5.2	34.6	Also called proline-rich protein 11. Uncharacterized.

212023_s_at	antigen identified by monoclonal antibody Ki-67	0.65	5.2	34.6	Antigen KI-67 is thought to be required for maintaining cell proliferation.
229442_at	chromosome 18 open reading frame 54	0.67	5.4	34.7	Uncharacterized
218663_at	chromosome condensation protein G	0.72	5.4	34.7	Member of the structural maintenance of chromosomes family of proteins; critical for DNA repair in mammals.
221436_s_at	cell division cycle associated 3	0.72	5.37	34.7	Tome-1 (trigger of mitotic entry 1) is a cytosolic protein required for proper activation of cdk1/cyclin B and mitotic entry.

Probeset represent the probe identifier as defined by Affymetrix, FC=fold change; q-value (%)=lowest false discovery rate at which a gene is described as significantly regulated; local FDR (%)=false discovery rate.

Supplementary Table S3: Top 20 up-regulated genes by prolonged (30 hours) 2-ME treatment identified by Significance Analysis of Microarrays.

Probeset	Gene product	FC	q-value (%)	localFDR (%)	Further information
206835_at	statherin	2.84	0	27.6	Statherin stabilises calcium phosphate in solution preventing spontaneous precipitation
206942_s_at	pro-melanin-concentrating hormone	1.62	0	27.4	Melanin-concentrating hormone (MCH) is a cyclic peptide originally identified as a circulating hormone in teleost fish, where it is secreted by the pituitary in response to stress and environmental stimuli. Expression/function in muscle is unknown.
235238_at	rai-like protein	1.40	0	26.8	SHC (Src homology 2 domain containing) family, member 4. It may serve as phosphotyrosine adaptor molecule in receptor-mediated signaling pathways.
221805_at	neurofilament, light polypeptide 68kDa (NF-L)	1.80	0	26.8	Neurofilaments are a class of intermediate filaments that comprise the major cytoskeletal component of differentiated neurons. During embryonic development, NF-L is expressed also in muscle.
205960_at & 225207_at	pyruvate dehydrogenase kinase, isoenzyme 4	1.59	0	26.5	Increased PDK4 expression suppresses glycolysis and enhance oxidation of fatty acids via inactivation of the pyruvate dehydrogenase complex
217475_s_at	LIM domain kinase 2	1.44	3.1	26.4	It phosphorylates cofilin, inhibiting its actin-depolymerizing activity. It is thought that this pathway contributes to Rho-induced reorganization of the actin cytoskeleton.
221577_x_at	growth differentiation factor 15	1.51	3.1	26.3	Member of the transforming growth factor-beta superfamily. It may regulate tissue

					differentiation and maintenance.
209301_at	carbonic anhydrase II	1.64	3.1	26.3	This enzyme determines the rate of conversion of carbon dioxide to carbonic acid and bicarbonate. Defects in this enzyme are associated with osteopetrosis (abnormally dense bone, due to defective resorption)
210118_s_at	interleukin 1, alpha	1.78	3.1	26.3	Endogenous interleukin-1 alpha promotes a proliferative and proinflammatory phenotype in human vascular smooth muscle cells.
216379_x_at & 266_s_at	CD24 antigen	1.64	3.1	26.3	It mediates the binding of monocytic cells and neutrophils to P-selectin.
203700_s_at	deiodinase, iodothyronine, type II	1.52	7.1	26.7	Local bioactive 3,3',5-triiodothyronine (T3) generation from thyroxine (T4) by Type II iodothyronine deiodinase in SMCs may play a role in anti-atherogenic effects of thyroid hormones.
1554290_at	hect domain and RLD 3	1.36	7.1	26.8	HERC3 may play a role in vesicular trafficking and its association with ubiquitin suggests that it may regulate ubiquitin-dependent processes.
234300_s_at	zinc finger protein 28 homolog (mouse)	1.45	7.5	26.9	Also known as KOX24. May be involved in transcriptional regulation.
205239_at	amphiregulin (schwannoma-derived growth factor)	1.65	7.5	27.1	It could be a potent growth factor for proliferative vascular diseases as it induces upregulation of cyclin D1 in VSMCs..

219263_at	ring finger protein 128	1.41	7.5	27.3	Also called GRAIL (gene related to anergy in lymphocytes), it is an E3 ubiquitin ligase that inhibits cytokine gene transcription
210997_at	hepatocyte growth factor; scatter factor	1.39	9.2	27.5	Hepatocyte growth factor induces vascular smooth muscle cell migration mediated by β 1 integrins and depending on PI3K activation..
206049_at	selectin P (CD62P)	1.35	9.6	27.9	The adhesion molecule P-selectin has been observed in VSMCs after vascular injury.
204834_at	fibrinogen-like 2 (fibroleukin)	1.43	9.6	27.9	Also known as fg12 prothrombinase, belongs to the fibrinogen family of proteins. Fgl2 prothrombinase has been shown to have the attributes of a serine protease capable of directly cleaving prothrombin to thrombin, leading to fibrin deposition.
1555872_a_at	hypothetical protein MGC21881	1.37	9.6	27.9	unknown

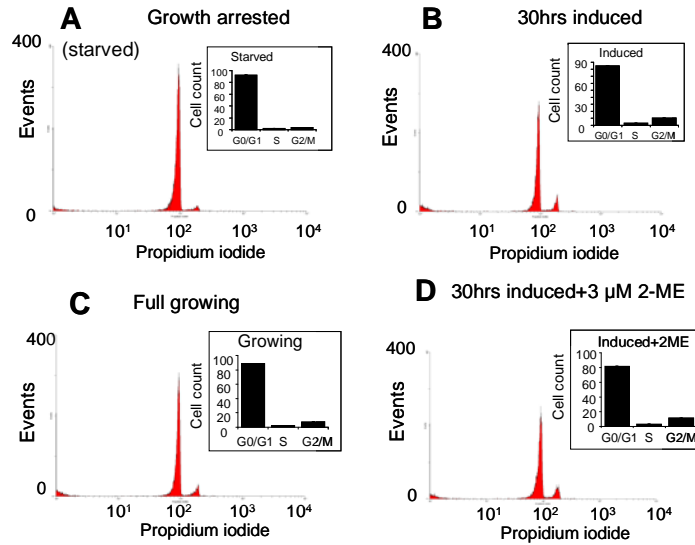
Probeset represent the probe identifier as defined by Affymetrix, FC=fold change; q-value (%)=lowest false discovery rate at which a gene is described as significantly regulated; local FDR (%)=false discovery rate.

Supplemental Table S 4 : Depicts the IC50 values for the binding of PPAR ligands and 2-ME in a competitive binding assay for PPAR- γ , PPAR- α , and PPAR- δ .

Binding Results :

	Roche Compound	Alpha IC50 (μ M)	Delta IC50 (μ M)	Gamma IC50 (μ M)
Ref. alpha	RO0728804	0.012	-----	-----
Ref. delta	RO4594390	-----	0.001	-----
Ref. gamma	RO2060257	-----	-----	0.002
	2-Methoxyestradiol	>10	>10	> 10

Supplemental Figure S1 : Modulatory effects of 2-ME on cell cycle distribution in serum starved and growing HASMCs.



% cell population	G ₀ /G ₁	S	G ₂ /M
A. Growth arrested	92.38±0.62	1.7±0.06	3.48±0.18
B. 30 hrs induced	84.95±0.27	2.92±0.18	10.46±0.29
C. Full growing	88.45±0.26	1.98±0.08	7.7±0.49
D. 30hrs 3µM 2ME	81.66±0.22	3.06±0.52	3.06±0.52

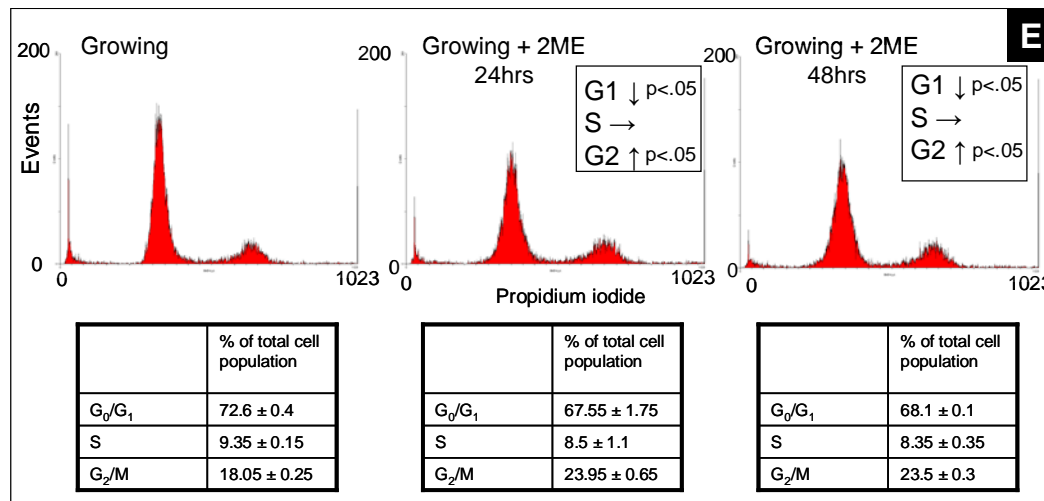
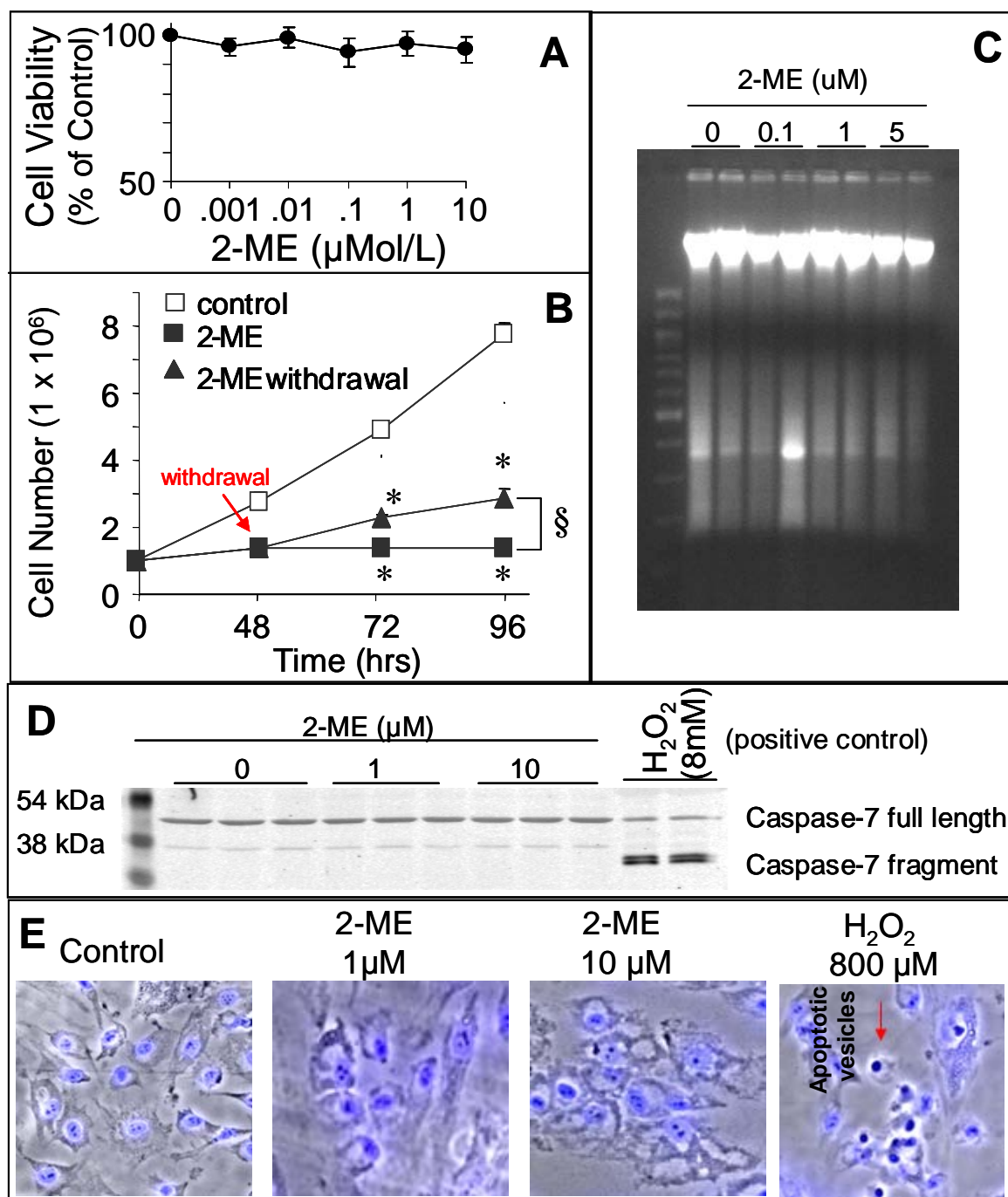
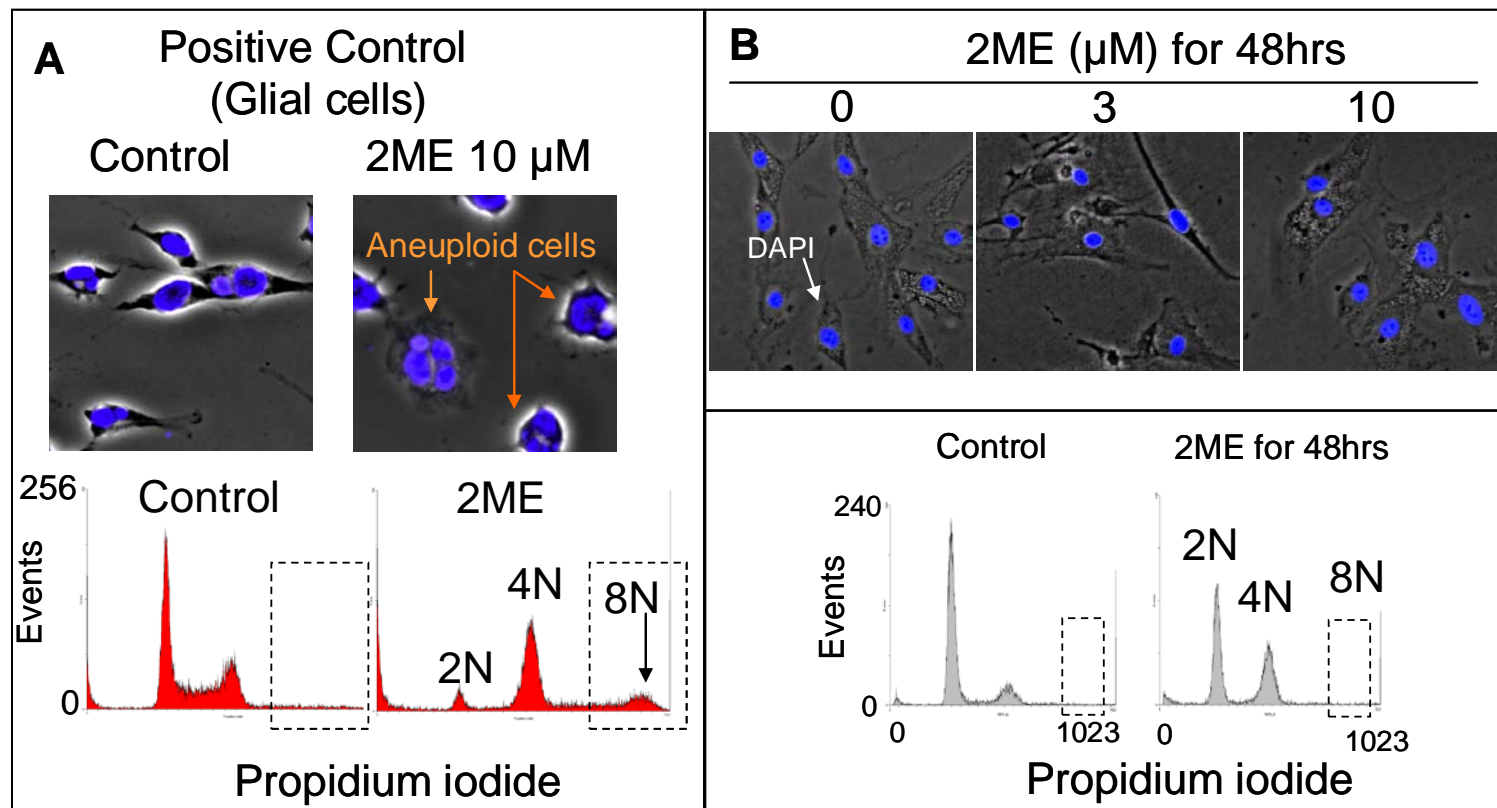


Figure S1 Legend: FACS Analysis showing cell cycle distribution under various conditions. Panel A depicts cell cycle distribution in serum starved HASMCs. Serum depletion induced accumulation of cells in G0/G1 phase (A). After 30 hrs of growth stimulation using 5% FCS (B), the cells escaped from the G0/G1 arrest (as shown by the decrease of the peak, from 92.38 ± 0.62 to 84.95 ± 0.27) and progressed through the S-phase into the G2/M phase (as indicated by the increase of the peak, from 3.48 ± 0.18 to 10.46 ± 0.29). The cell cycle distribution following 30 hrs of growth induction is comparable to the one of full proliferating cells (C). However, a slightly difference in the high of the G2/M peak (10.46 ± 0.29 versus 7.7 ± 0.49 in growth stimulated versus full growing cells, respectively) may indicate that after 30 hrs of stimulation, the cells are still partially synchronized. Eventhough 2-ME inhibits HASMC growth, the presence of $3 \mu\text{M}$ 2-ME after 30 hrs did not alter the cell cycle distribution (D) with respect to its control (B), more importantly, in growing cells 2-ME significantly altered cell cycle distribution after 24 and 48 hrs of treatment. It significantly inhibited G0/G1 phase (from $72.6 \pm 0.4\%$ to $67.55 \pm 1.75\%$) and significantly induced G2/M phase (from $18.05 \pm 0.25\%$ to $23.95 \pm 0.65\%$) (**Panel E**). This suggests that 2-ME arrests HASMC growth via double blockade of cell cycle.

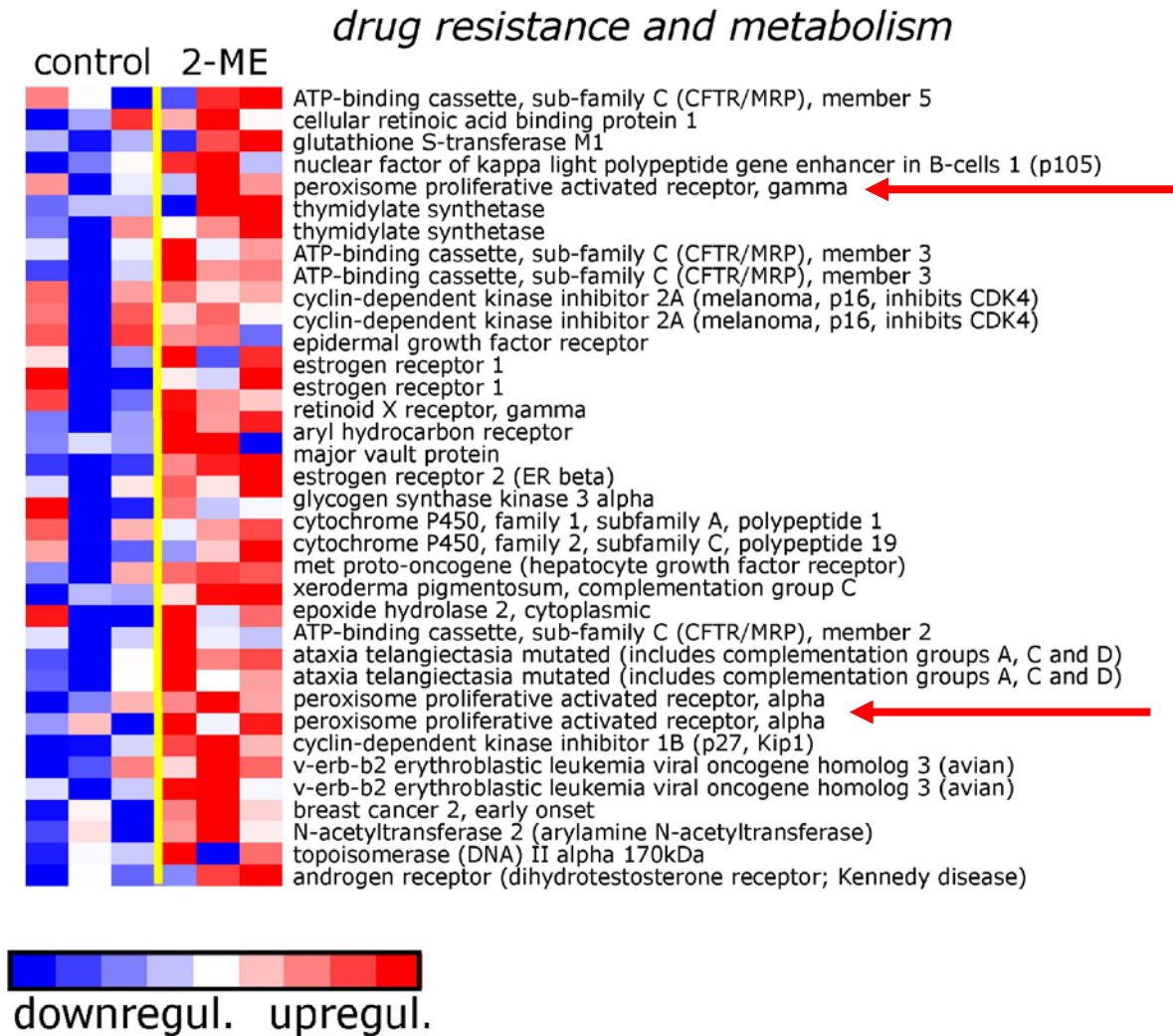
Figure S2: Line graph, photomicrographs and representative gels showing the effects of 2-ME on SMC Viability and Apoptosis. Treatment with 2-ME did not result in loss of cell viability (trypan blue exclusion; A), moreover there was no cell loss and cells regained growth after 2-ME withdrawal (B). 2-ME treatment did not induce DNA fragmentation (C), caspase 7 fragmentonn (D), or formation of apoptotic vesicles (E). In cells treated with H₂O₂ (positive control)apoptosis was observed. § p<.05 significant reversal; * p<.05 vs control.



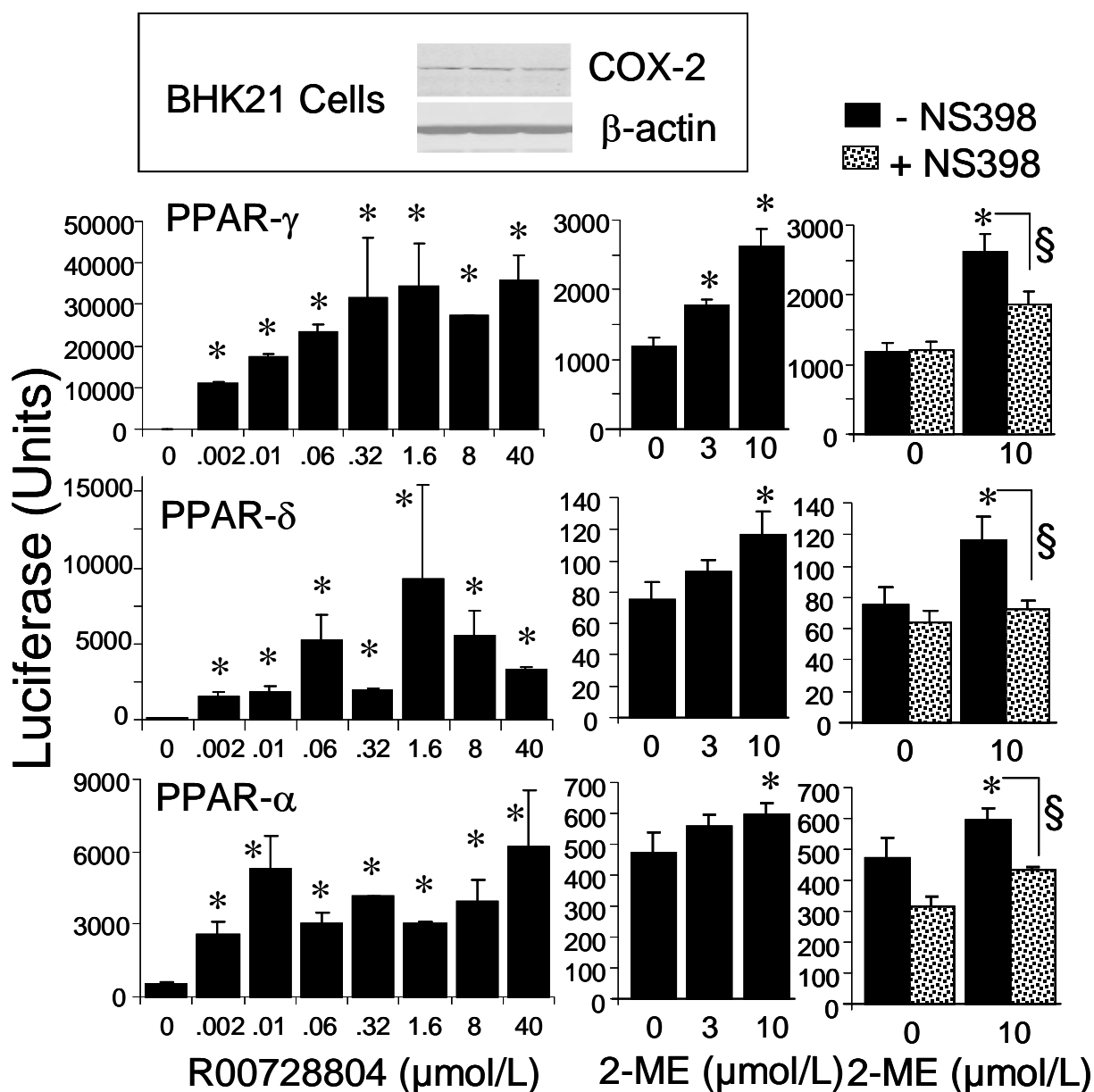
Supplemental Figure S3: Effects of 2-ME on aneuploidy. Treatment of Glial / oligodendrocytes (A) or HASMCs with 2-ME 3-10 $\mu\text{mol/L}$ for 48 hrs under growing conditions induced endoreduplication / aneuploidy in glial , but not HASMCs. Panel A shows photomicrograph of aneuploid cells as well as flow cytometric histogram with a peak of 8N (multinucleated cells) in 2-ME treated cells. Similar treatment of HASMCs did not result in aneuploid cells nor presence of 8N cells (B).



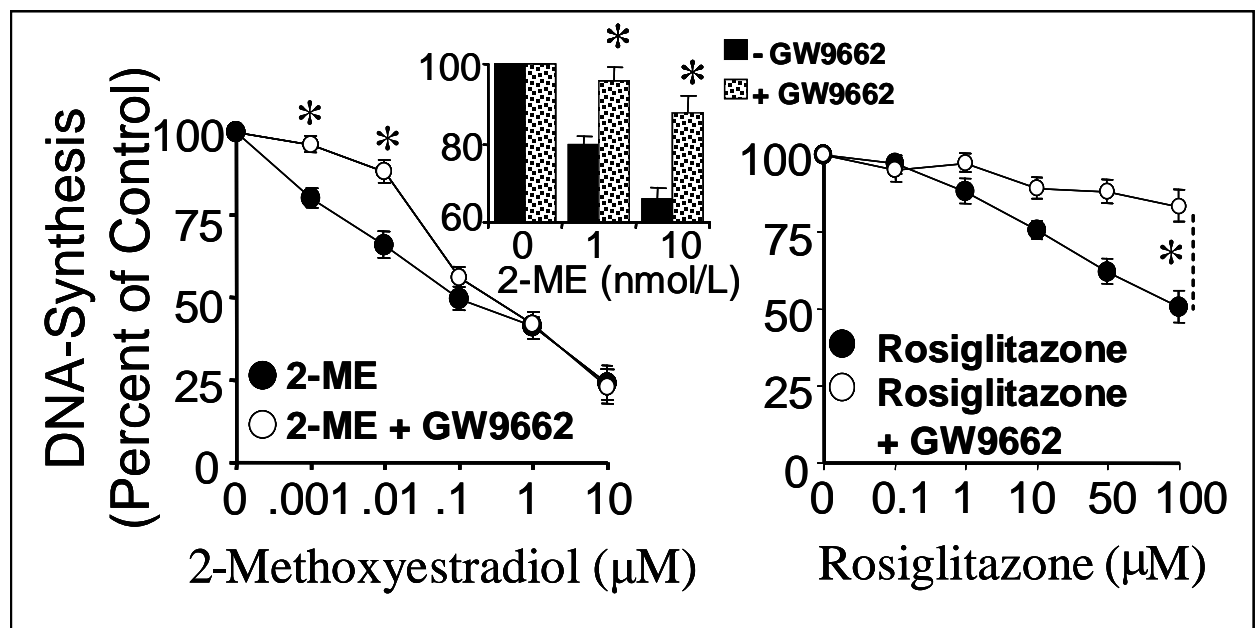
Supplemental Figure S4: 2-ME upregulates PPAR- γ and PPAR- α genes in HASMCs within the genes for drug resistance and metabolism. Arrows indicate upregulation of PPAR gamma and alpha receptors.



Supplemental Figure S5 : Bar graph comparing the effects of 2-ME and known PPAR ligand (RO00728804) on PPAR- γ , PPAR- α and PPAR- δ activation. Right panels demonstrate the modulatory effects of 2-ME in cells pretreated with or without COX-2 inhibitor NS-398 (10 μ mol/L) for 6hrs. Representative photomicrograph depicts the presence of COX-2 in BHK21 cells. * $p < .05$ vs vehicle treated control; § $p < .05$ significant reversal vs 2-ME.



Supplemental Figure S6: Depicts the attenuation by PPAR γ antagonist, GW9662, of the concentration-dependent inhibitory effects of 2-ME (0.001-10 $\mu\text{mol/L}$; left panels) or rosiglitazone (0.1-100 $\mu\text{mol/L}$; right panels) on 2.5% FCS-induced DNA synthesis in human aortic SMCs. Data represents mean \pm SEM from 3 separate experiments conducted in triplicates. * $p < 0.05$ significant reversal of the inhibitory effects of 2-ME or rosiglitazone by GW9662.



Supplementary Figure S7: Depicts the modulatory effects of GW9662 ($\mu\text{mol/L}$) on 2-ME ($10\mu\text{mol/L}$) induced COX-2 expression in HASMCs treated for 48 hours. * $P < 0.05$ versus vehicle treated control; § no significant induction versus vehicle treated control (Cont).

